18

Standard Mass Matrices For Plane Beam Elements

TABLE OF CONTENTS

§18.1. The Plane BE Beam

The two-node plane BE-beam element has length ℓ, cross section area A and uniform mass density ρ. Only the translational inertia due to the lateral motion of the beam is considered in the kinetic energy $T = \frac{1}{2}\int_0^\ell \rho\dot{v}(\bar{x})^2\,d\bar{x}$ of the element, whereas its rotational inertia is ignored. The freedoms are arranged as $\mathbf{u}^e = [\,v_1\;\;\theta_1\;\;v_2\;\;\theta_2\,]^T$. The natural coordinate ξ varies from $\xi = -1$ at node 1 ($x = 0$) to $\xi = +1$ at node 2 ($x = \ell$), whence $dx/d\xi = \frac{1}{2}\ell$ and $d\xi/dx = 2/\ell$. The well known cubic shape functions in terms of ξ are collected in the shape function matrix

$$\mathbf{N}^e = [\,\tfrac{1}{4}(1-\xi)^2(2+\xi)\quad \tfrac{1}{8}\ell(1-\xi)^2(1+\xi)\quad \tfrac{1}{4}(1+\xi)^2(2-\xi)\quad -\tfrac{1}{8}\ell(1+\xi)^2(1-\xi)\,] \tag{18.1}$$

The CMM obtained by analytical integration is

$$\mathbf{M}^e_{CMM} = \rho A\int_{-1}^{1} J\,(\mathbf{N}^e)^T\mathbf{N}^e\,d\xi = \frac{m^e}{420}\begin{bmatrix} 156 & 22\ell & 54 & -13\ell \\ 22\ell & 4\ell^2 & 13\ell & -3\ell^2 \\ 54 & 13\ell & 156 & -22\ell \\ -13\ell & -3\ell^2 & -22\ell & 4\ell^2 \end{bmatrix}. \tag{18.2}$$

in which the Jacobian $J = dx/d\xi = \ell/2$ and $m^e = \rho\,A\,\ell$. The mass matrices obtained with Gauss integration rules of 1, 2 and 3 points are

$$C_1\begin{bmatrix} 16 & 4\ell & 16 & -4\ell \\ 4\ell & \ell^2 & 4\ell & -\ell^2 \\ 16 & 4\ell & 16 & -4\ell \\ -4\ell & -\ell^2 & -4\ell & \ell^2 \end{bmatrix},\; C_2\begin{bmatrix} 86 & 13\ell & 22 & -5\ell \\ 13\ell & 2\ell^2 & 5\ell & -\ell^2 \\ 22 & 5\ell & 86 & -13\ell \\ -5\ell & -\ell^2 & -13\ell & 2\ell^2 \end{bmatrix},\; C_3\begin{bmatrix} 444 & 62\ell & 156 & -38\ell \\ 62\ell & 11\ell^2 & 38\ell & -9\ell^2 \\ 156 & 38\ell & 444 & -62\ell \\ -38\ell & -9\ell^2 & -62\ell & 11\ell^2 \end{bmatrix}, \tag{18.3}$$

in which $C_1 = m^e/64$, $C_2 = m^e/216$ and $C_3 = m^e/1200$. Their eigenvalue analysis shows that all three are singular, with rank 1, 2 and 3, respectively. The result for 4 and more points agrees with (18.2), which has full rank. The main purpose of this example is to illustrate the rank property stated in §16.6: each Gauss point adds one to the rank up to 4, since the problem is one-dimensional.

The matrix (18.2) conserves linear and angular momentum. So do the reduced-integration mass matrices (18.3) if the number of Gauss points is 2 or greater.

To get a diagonally lumped mass matrix is trickier. Obviously the translational nodal masses must be the same as that of a bar: $\frac{1}{2}\rho A\ell$. See Figure 18.1. But there is no easy road on rotational masses. To accommodate these variations, it is convenient to leave the latter parametrized as follows

$$\bar{\mathbf{M}}^e_L = m^e\begin{bmatrix} \frac{1}{2} & 0 & 0 & 0 \\ 0 & \alpha\ell^2 & 0 & 0 \\ 0 & 0 & \frac{1}{2} & 0 \\ 0 & 0 & 0 & \alpha\ell^2 \end{bmatrix},\quad \alpha \ge 0. \tag{18.4}$$

Here α is a nonnegative parameter, typically between 0 and 1/100. The choice of α has been argued in the FEM literature over several decades, but the whole discussion is largely futile. Matching the angular momentum of the beam element gyrating about its midpoint gives $\alpha = -1/24$. This violates the positivity condition. It follows that the *best possible* α — as opposed to possible best — is zero. This choice gives, however, a singular mass matrix. This is undesirable in scenarios where a mass-inverse appears.

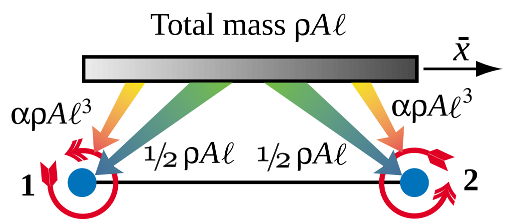

FIGURE 18.1. Direct mass lumping for two-node plane BE beam element.

This result can be readily understood physically. The $m^e/2$ translational end node masses grossly overestimate (in fact, by a factor of 3) the angular momentum of the element. Hence adding any rotational lumped mass only makes things worse.

§18.2. The Plane Timoshenko Beam

The Timoshenko beam (Ti-beam) incorporates two refinements over the Bernoulli-Euler (BE) model:

1. For both statics and dynamics: plane sections remain plane but not necessarily normal to the deflected midsurface. See Figure 24.4 for the kinematics. This assumption allows the averaged shear distortion to be included in both strain and kinetic energies.
2. In dynamics: the rotary inertia is included in the kinetic energy.

This model is more important for dynamics and vibration than BE, and indispensable for rapid transient and wave propagation analysis. More specifically, the BE beam has infinite phase velocity, because the EOM is parabolic, and thus becomes useless for high-fidelity wave propagation.

According to the second assumption, the kinetic energy of the Ti-beam element is given by

$$T = \tfrac{1}{2} \int_0^\ell \left(\rho A\, \dot{v}(x)^2 + \rho I_R\, \dot{\theta}(x)^2 \right) dx. \tag{18.5}$$

Here I_R is the second moment of inertia to be used in the computation of the rotary inertia and $\theta = v' + \gamma$ is the cross-section rotation angle shown in Figure 24.4; $\gamma = V/(GA_s)$ being the section-averaged shear distortion. The element DOF are ordered $\mathbf{u}^e = [\, v_1 \;\; \theta_1 \;\; v_1 \;\; \theta_2 \,]^T$. The lateral displacement interpolation is

$$v(\xi) = v_1 N^e_{v1}(\xi) + v'_1 N^e_{v'1}(\xi) + v_2 N^e_{v2}(\xi) + v'_2 N^e_{v'2}(\xi), \qquad \xi = \frac{2x}{\ell} - 1, \tag{18.6}$$

in which cubic interpolation functions are used. A complication over BE is that the rotational freedoms are θ_1 and θ_2 but the interpolation (18.6) is in terms of the neutral surface end slopes: $v'_1 = (dv/dx)_1 = \theta_1 - \gamma$ and $v'_2 = (dv/dx)_2 = \theta_2 - \gamma$. From a kinmatic analysis we can derive the relation

$$\begin{bmatrix} v'_1 \\ v'_2 \end{bmatrix} = \frac{1}{1+\Phi} \begin{bmatrix} -\frac{\Phi}{\ell} & 1+\frac{\Phi}{2} & \frac{\Phi}{\ell} & -\frac{\Phi}{2} \\ -\frac{\Phi}{\ell} & -\frac{\Phi}{2} & \frac{\Phi}{\ell} & 1+\frac{\Phi}{2} \end{bmatrix} \begin{bmatrix} v_1 \\ \theta_1 \\ v_2 \\ \theta_2 \end{bmatrix}, \tag{18.7}$$

in which the dimensionless parameter $\Phi = 12EI/(GA_s\,\ell^2)$ characterizes the ratio of bending and shear rigidities. The end slopes of (18.7) are replaced into (18.6), the interpolation for θ obtained, and v and θ inserted into the kinetic energy (18.5).

After lengthy algebra the CMM emerges as the sum of two contributions:

$$
\begin{aligned}
&\mathbf{M}^e_{CMM} = \mathbf{M}^e_{CT} + \mathbf{M}^e_{CR} = \\
&C_T \begin{bmatrix}
\frac{13}{35}+\frac{7}{10}\Phi+\frac{1}{3}\Phi^2 & (\frac{11}{210}+\frac{11}{120}\Phi+\frac{1}{24}\Phi^2)\ell & \frac{9}{70}+\frac{3}{10}\Phi+\frac{1}{6}\Phi^2 & -(\frac{13}{420}+\frac{3}{40}\Phi+\frac{1}{24}\Phi^2)\ell \\
 & (\frac{1}{105}+\frac{1}{60}\Phi+\frac{1}{120}\Phi^2)\ell^2 & (\frac{13}{420}+\frac{3}{40}\Phi+\frac{1}{24}\Phi^2)\ell & -(\frac{1}{140}+\frac{1}{60}\Phi+\frac{1}{120}\Phi^2)\ell^2 \\
 & & \frac{13}{35}+\frac{7}{10}\Phi+\frac{1}{3}\Phi^2 & (\frac{11}{210}+\frac{11}{120}\Phi+\frac{1}{24}\Phi^2)\ell \\
\text{symmetric} & & & (\frac{1}{105}+\frac{1}{60}\Phi+\frac{1}{120}\Phi^2)\ell^2
\end{bmatrix} \\
&+ C_R \begin{bmatrix}
\frac{6}{5} & (\frac{1}{10}-\frac{1}{2}\Phi)\ell & -\frac{6}{5} & (\frac{1}{10}-\frac{1}{2}\Phi)\ell \\
 & (\frac{2}{15}+\frac{1}{6}\Phi+\frac{1}{3}\Phi^2)\ell^2 & (-\frac{1}{10}+\frac{1}{2}\Phi)\ell & -(\frac{1}{30}+\frac{1}{6}\Phi-\frac{1}{6}\Phi^2)\ell^2 \\
 & & \frac{6}{5} & (-\frac{1}{10}+\frac{1}{2}\Phi)\ell \\
\text{symmetric} & & & (\frac{2}{15}+\frac{1}{6}\Phi+\frac{1}{3}\Phi^2)\ell^2
\end{bmatrix}.
\end{aligned}
\tag{18.8}
$$

in which $C_T = \rho\,A\,\ell/(1+\Phi)^2 = m^e/(1+\Phi)^2$ and $C_R = \rho\,I_R/((1+\Phi)^2\,\ell)$. Matrices $\mathbf{M}_{CT}$ and $\mathbf{M}_{CR}$ account for translational and rotary inertia, respectively. Caveat: the I in $\Phi = 12EI/(GA_s\,\ell^2)$ is the second moment of inertia that enters in the elastic flexural elastic rigidity. If the beam is homogeneous $I_R = I$, but that is not necessarily the case if, as sometimes happens, the beam has nonstructural attachments that contribute rotary inertia.

The scale factor of $\mathbf{M}^e_{CR}$ can be further transformed to facilitate parametric studies by introducing $r_R^2 = I_R/A$ as cross-section gyration radius and $\Psi = r_R/\ell$ as element slenderness ratio. Then $C_R = \rho I_R/((1+\Phi)^2\,\ell) = \rho A\,\ell\,\Psi^2/(1+\Phi)^2 = m^e\,\Psi^2/(1+\Phi)^2$. If $\Phi = 0$ and $\Psi = 0$, $\mathbf{M}^e_{CR}$ vanishes and $\mathbf{M}^e_{CT}$ in (18.8) reduces to (18.2).

A DLMM can be obtained through the HRZ scheme explained in §D.1. The optimal lumped mass is derived in §24.2.5 via templates.